Influence of porosity on the fatigue behaviour of welded joints

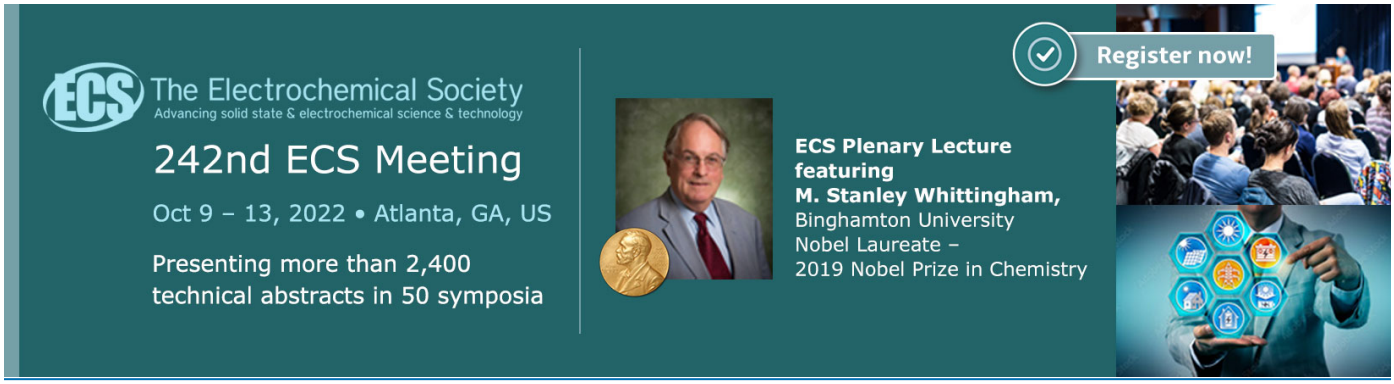

Influence of porosity on the fatigue behaviour of welded joints

P Livieri, R Tovo

Dept of Engineering, University of Ferrara, via Saragat 1, 44122, Ferrara, Italy

E-mail: paolo.livieri@unife.it

Abstract. In this paper, the influence of a single pore on the fatigue behaviour of welded joints has been examined by means of the implicit gradient approach. The pore has been considered a stress raiser that interacts with the weld toe or weld root. As an example, in the case of a cruciform joint with a load-carrying fillet weld, the influence of a single spherical pore is examined. Furthermore, the fatigue behaviour of an aluminium laser welded joint with ellipsoid equivalent pores is considered and a comparison is made with the fatigue strength of an aluminium arc welded joint.

1. Introduction

The presence of defects in welded joints reduces their strength performance such that the dimensions of the defects must be taken into account as underlined in many documents including ISO 6520 *Classification of imperfections in metallic fusion welds* [1], ISO 5817 [2] and ISO 10042 [3]. From a design point of view, in reference [4], Hobbacher classified defects into different categories such as imperfect shape (linear misalignment and angular distortions), undercuts, volumetric discontinuities (gas pore and cavities of any shape), and planar discontinuities (lack of fusion or lack of penetration). For instance, in the case of porosity, the limitations are given in terms of the percentage of the porosity area on the radiograph or as the maximum pore diameter or width smaller than ¼ plate thickness or 6 mm. These rules are valid for both steel and aluminium welds. From an analytical point of view, in the literature, the assessments of the fatigue life of components weakened by defects can be treated by considering an equivalent defect. The flaw can be considered as an elliptical or semi elliptical crack [4, 5, 6], and then, by means of linear fracture mechanics, the propagation of defects is considered of fundamental importance for fatigue life estimation [7, 8, 9]. Alternatively, the endurance limit of the material with defects can be estimated by considering Murakami's equivalent crack length method [10] in relation to the square root of the *area* defects [11, 12, 13]. In both procedures, it has been assumed that three-dimensional defects are reduced to a two-dimensional form by an appropriate projection of the actual defect with the loss of some three-dimensional features. For instance, as recently underlined in reference [14], the critical defects could not be simply identified by the critical value related to the square root of its projected area.

This paper could be considered as a preliminary work that examines the problem of porosity in welded joints by means of the implicit gradient approach. It considers a single pore of spherical or ellipsoidal form that interacts with other stress raisers such as the weld root or weld toe. The pore is considered with its three-dimensional form and a preliminary parametric FE analysis has been proposed. Finally, as an example, the fatigue behaviour of an aluminium laser welded joint with ellipsoid equivalent pores is considered and a comparison is made in terms of fatigue strength with aluminium arc welded joints.

2. The implicit gradient approach

The total fatigue life of a welded component could be evaluated by means of the implicit gradient approach as proposed in previous papers [15, 16]. This approach evaluates the effective stress σ_{eff} correlated to the average stress around the stress raiser where the fatigue crack nucleates and propagates up to final failure.

For a welded joint, and by using Williams' equations [17], the asymptotic local stress field can be described with the help of notch stress intensity factors (NSIF, see ref. [18]). If the opening angle is greater than 102° and only mode I is singular, the effective stress, σ_{eff}, relates to the average stress fields generated by a stress raiser such as a sharp V-notch and can be analytically estimated by using the implicit gradient method as [19]:

$$\sigma_{eff} = \frac{m_v}{c^{1-\lambda_1}} K_{N,1} \tag{1}$$

where m_v is a non-dimensional parameter that depends only on the opening angle and λ_1 is Williams' eigenvalue of mode I (for $2\alpha=0$ and 135°, λ_1 assumes the values of 0.5 and 0.674, respectively). The parameter m_v is equal to 0.405 for 2α, which is equal to 135°. The characteristic length c is assumed constant and related only to the type of material (c=0.2 mm for steel welded joints and c=0.15 for aluminium welded joints [20]).

In general, the effective stress can be numerically evaluated after solving the classical FE analysis. For welded joints, the Cauchy principal stress is the input for solving the Helmholz differential equation proposed in [21] for the assessment of the effective stress [22] (see Appendix A for essential analytical details).

As an example, Figure 1 shows the effective stress in the case of a cruciform joint with a load carrying weld. The main plate has a thickness of 20 mm and a tensile loading is applied at the remote nominal section. The dimensions of the joints are reported in the Figure as well as the effective stress with a colour scale. In this example, the maximum effective stress at the weld toe is on the longitudinal symmetry plane, whereas, at the weld root, the maximum is in the neighbourhood of the plate border as indicated in Figure 2.

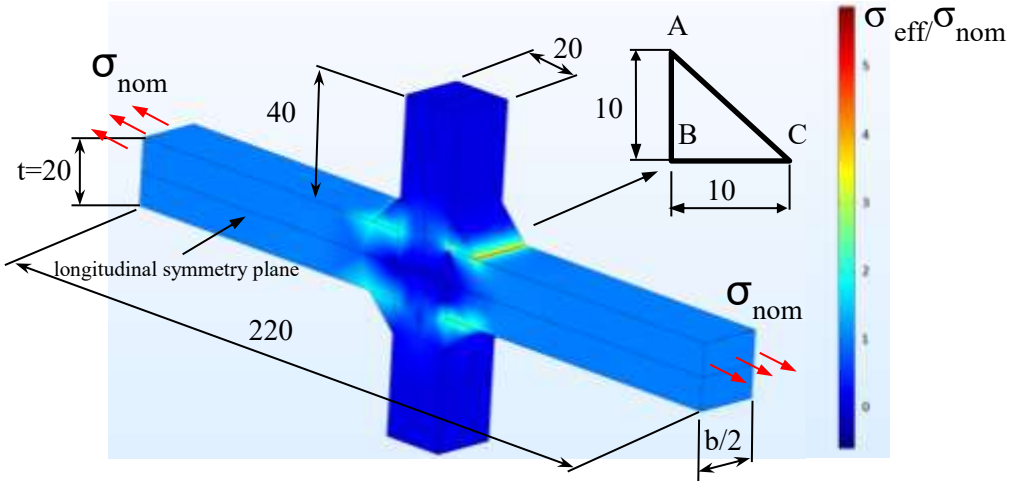

Figure 1. Effective stress in dimensionless form for a load carrying welded joint under axial loading σ_{nom} (c=0.2 mm, b= 40 mm)

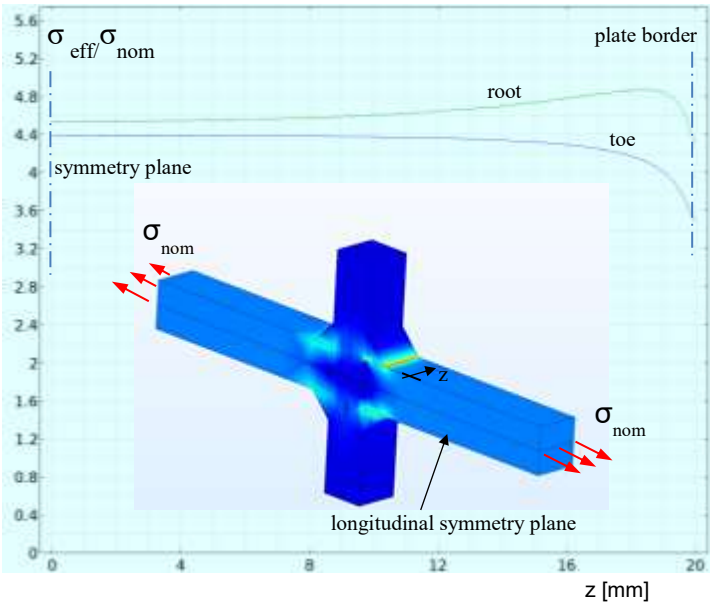

Figure 2. Effective stress in dimensionless form for the load carrying welded joint in Figure 1 along the weld root and weld toe. z is zero at the longitudinal symmetry plane (c=0.2 mm)

3. Numerical analysis of a load carrying welded joint

The numerical analysis of the welded joint in Figure 1 takes into account a spherical pore of a different diameter that moves inside the triangle ABC. Note that the maximum effective stress at the root is near the border of the weld whereas, at the toe, the maximum is located on the longitudinal symmetry plane. Furthermore, at the root, because the opening angle is close to zero, the maximum effective stress has slightly shifted from the root [19] and its value is equal to $\sigma_{eff,max} / \sigma_{nom} = 5.1$, which is very close to the maximum reported in Figure 2.

Figure 3 shows the effective stress when the pore moves along the bisector of the angle $A\widehat{B}C$ at the distance of 18 mm from the longitudinal symmetry plane. The pore is kept tangent to the primary and secondary plate of a thickness equal to 20 mm. The presence of the pore increases the value of the effective stress in the weld. Furthermore, an increment of the effective stress is also possible when the pore moves along the longitudinal symmetry axis. Figure 4 and 5 underline that, when the pore is near the root or at the toe, a magnification of the stress occurs and increases when the pore increase in size. In Figure 4, the pore is tangent to the primary plate.

The increasing in the effective stress could be correlated to the decrease in the fatigue strength of the material. The fatigue scatter band obtained for the weld in terms of effective stress could also be used for welds with pores even if the location of the maximum effective stress moves from the weld toe or root to the pore. This feature will be examined in the next section. In term of effective stress, a magnification of the $\sigma_{eff,max} / \sigma_{nom}$ is possible with a pore that is smaller than ¼ of the main plate size (see Figures 3–5).

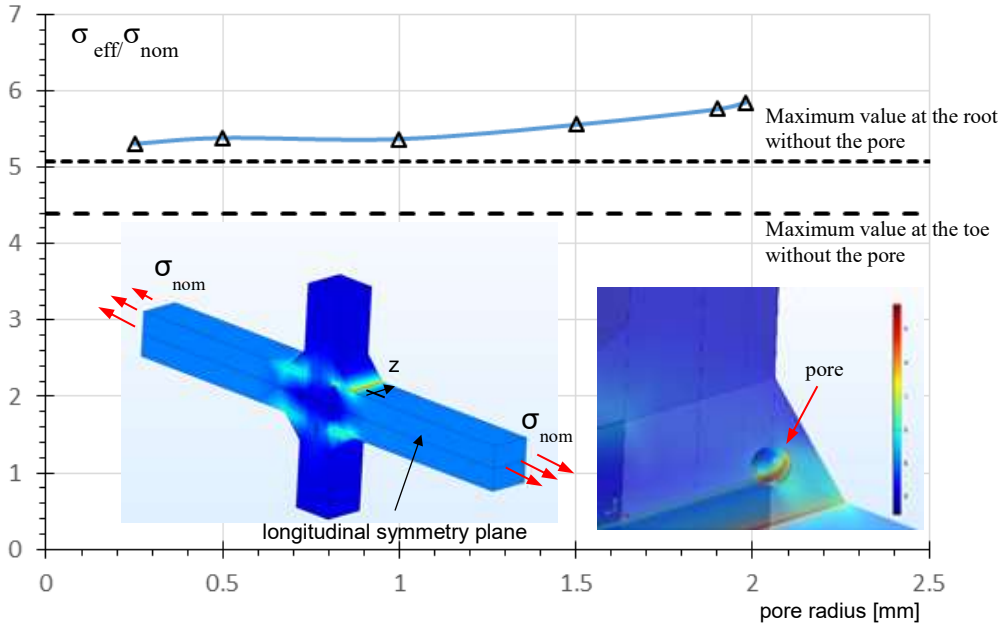

Figure 3. Effective stress in dimensionless form for the load carrying welded joint in Figure 1. The centre of the pore moves along the bisector of $A\hat{B}C$ at z= 18 mm and at the same time it is tangent to the segments AB and BC.

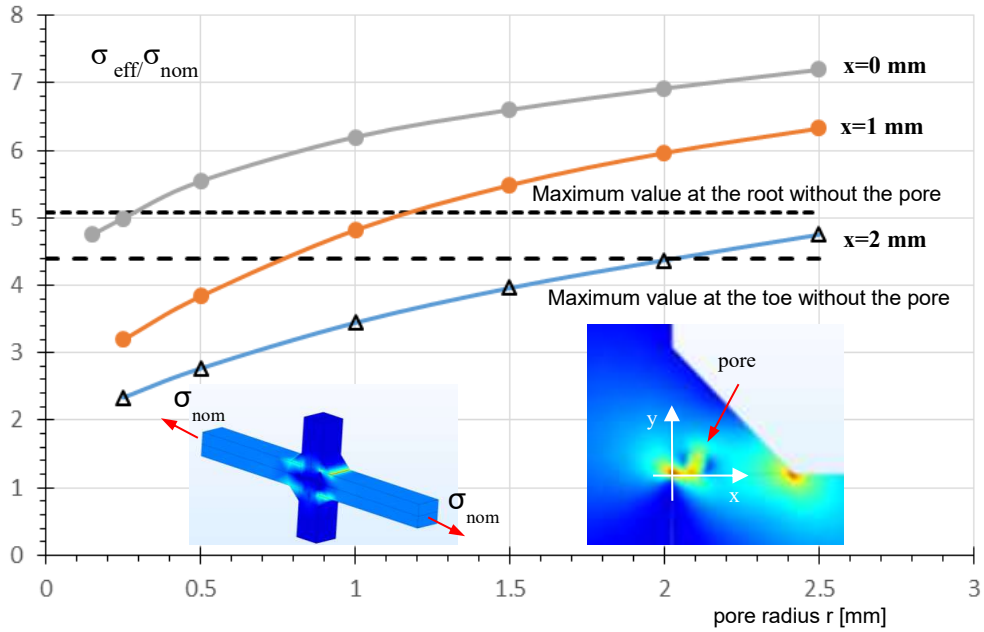

Figure 4. Effective stress in dimensionless form for the load carrying welded joint in Figure 1. The pore moves close to the root on the longitudinal symmetry plane z=0 mm and is tangent to the primary plate (c=0.2 mm).

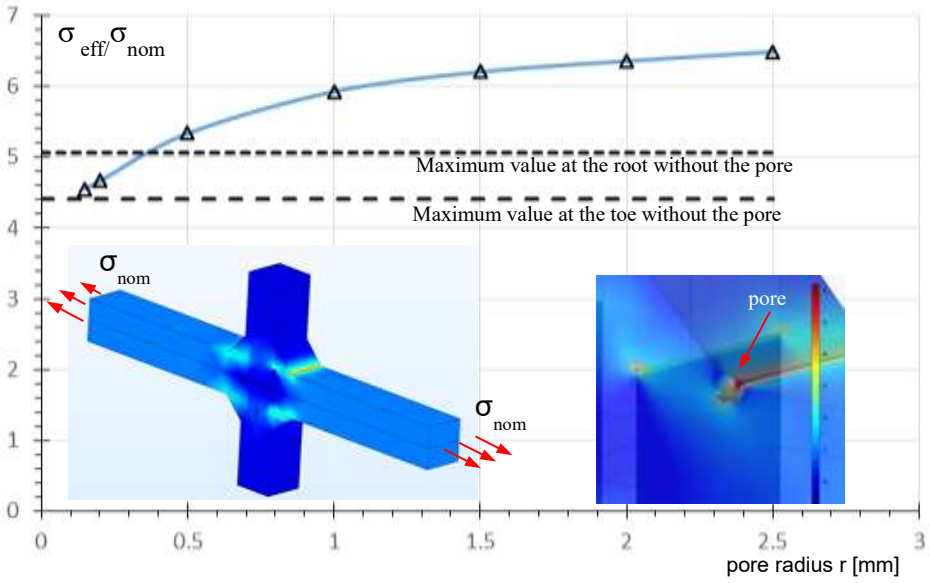

Figure 5. Effective stress in dimensionless form for the load carrying welded joint in Figure 1. The centre of the pore is located at the weld toe in the longitudinal symmetry plane (c=0.2 mm)

4. Fatigue life in laser welded joints with high porosity

In a previous paper, the experimental fatigue strength of two series of laser welded butt joints with large defects was evaluated [23]. The joints consisted of 5 mm thick 5083 H321 aluminium alloy plates, and the location, size and shape of the flaws were accurately determined by means of a micro and macro structural investigation of the joint after fatigue failure. Figure 6 shows an example of the location of the fracture surface and the surface after the fatigue test. The stress raising given by the defect was more significant than the weld toe. Most of the detected defects present in the specimens could be classified as cavities of inert gas that were trapped during the welding procedure and were approximately oriented at 45° (we noted that, based on standard UNI EN 26520 [1], the revealed defects can be classified as linear porosity and elongated cavity). Although this standard covers the arc-welding procedure, these types of defects are not acceptable whatever the considered quality level. The percentage porosity as measured on the fracture surface by means of suitable software dedicated to image analysis resulted in 33% and 26% for series A and B, respectively.

Due to the over-estimation of the equivalent flaw size by applying the assessment procedure as proposed in Ref. [4], an alternative method was developed in reference [23]. In particular, the pore dimensions were measured in a frame of reference parallel to its principal axes instead of along the main plate free edges, as shown in Figure 7. Doing so, a smaller equivalent flaw size was derived and the interaction criteria were modified according to the new frame of reference. After failure, a table with equivalent elliptical flaws was obtained for each specimen.

Now for the A series, by means of the implicit gradient approach, we evaluated the effective stress of the butt weld joint with equivalent defects inside the weld described as an ellipsoid of revolution inclined at 45°. For the sake of simplicity, all equivalent defects were considered but only one was considered at a time in each FE analysis. Each equivalent flaw was characterized by a different size *a,b* and position *p*. The pore was positioned on the symmetry plane of the weld as reported in Figure 8.

The maximum effective stress at the weld toe without the flaw is equal to $\sigma_{eff,max} / \sigma_{nom} = 1.1$. For each specimen, the FE analysis identifies the most critical flaw. The numerical analysis showed that the maximum effective stress $\sigma_{eff,max} / \sigma_{nom}$ ranges between 2.5 and 3.4. Figure 9, as an example, shows the trend of effective stress as a function of the arc length *s* along the weld toe, the plate and the equatorial

section of the defects. The presence of the defect locally increases the effective stress on the plate and on the weld toe but the maximum value is ratchets on the defects. So doing, for each specimen the critical flaw was identified as the flaw with the maximum value of $\sigma_{eff,max} / \sigma_{nom}$.

Figure 10 reports, for the critical flaw, the range of maximum effective stress against the cycles to failure. The scatter band reported in the Figure is that of the arc welded aluminium alloy proposed in reference [20].

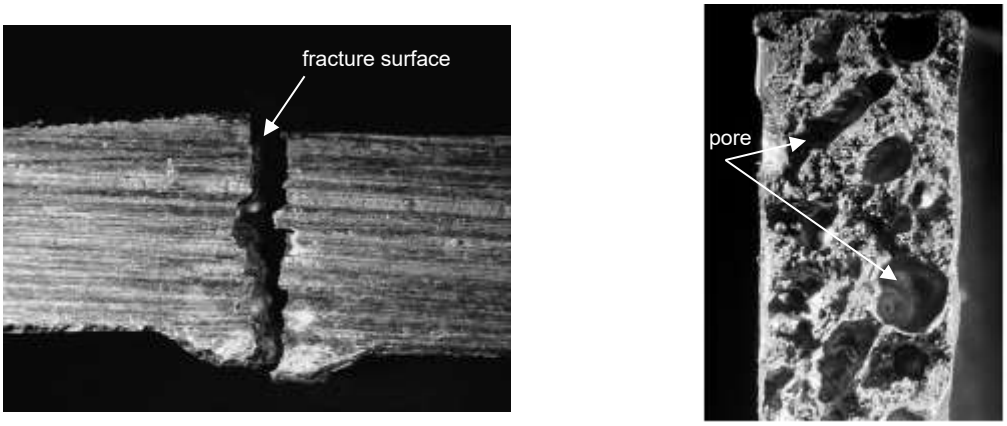

Figure 6. a) Location of the fracture surface in the weld bead; b) Fracture surface A series [23].

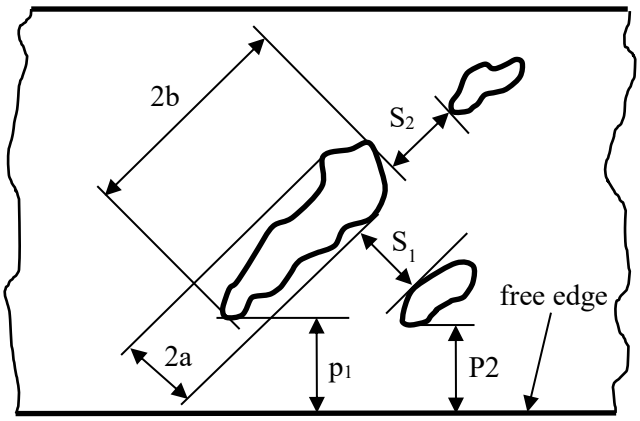

Figure 7. Revised criterion for flaw dimension measurement and flaw interaction [23].

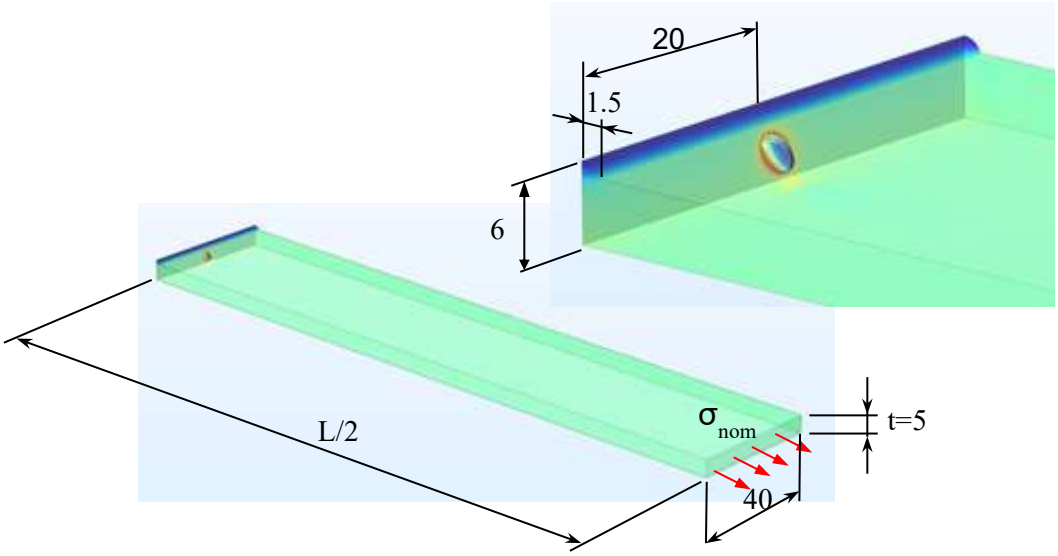

Figure 8. Effective stress in dimensionless form for a butt welded joint under axial loading σ_{nom} (c=0.15 mm, L= 400 mm)

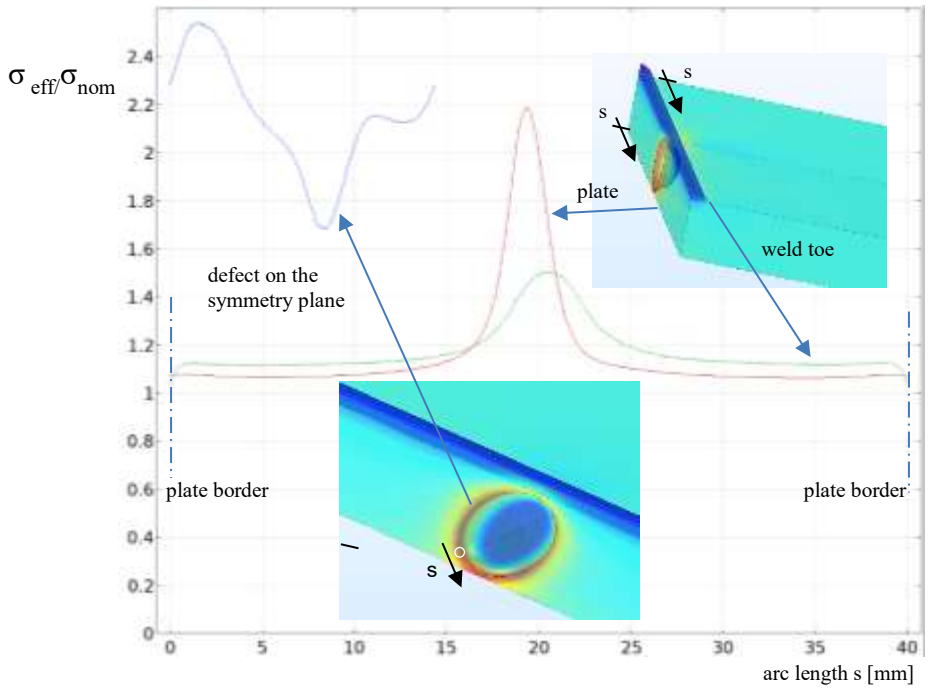

Figure 9. Effective stress on the welded joint with elliptical defects under remote uniform tensile loading σ_{nom} (c=0.15 mm, *s* is the arc length)

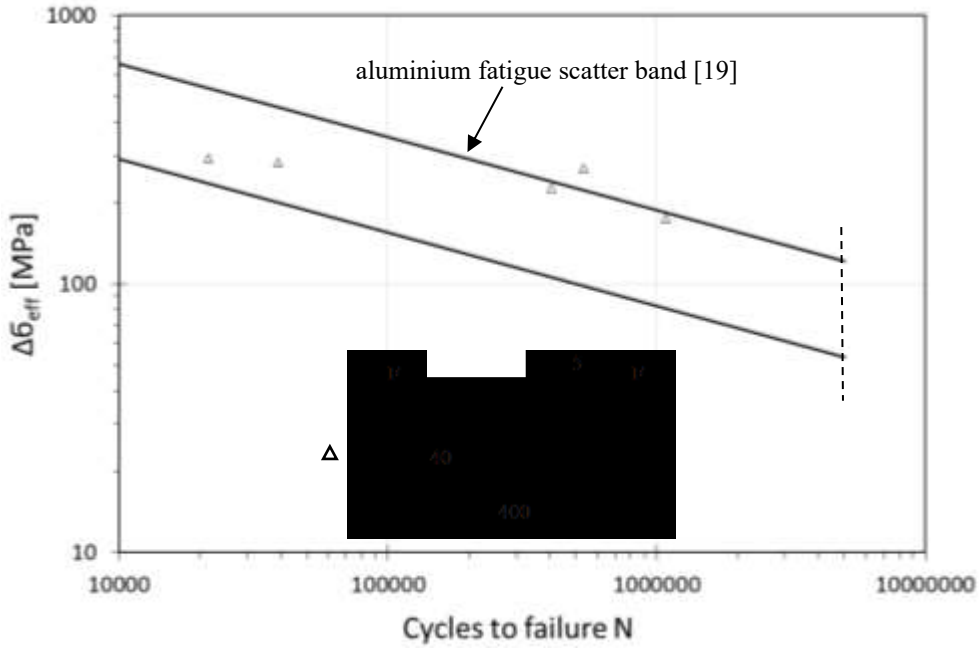

Figure 10. Range of maximum effective stress for a butt weld joint with an ellipsoidal equivalent defect under remote uniform tensile loading σ_{nom} (c=0.15 mm)

5. Conclusions

The three dimensional FE analysis in conjunction with the implicit gradient approach provide a useful tool suitable for studying the influence of porosity on the fatigue strength of welded joints. This is possible because the weld imperfections can be considered as geometrical variables. The implicit approach gives us the effect of the stress concentration on the weld root or weld toe as well as on the surface of the pore inside the welded metal. The presence of the pore can increase the fatigue stress concentration factor while decreasing the fatigue strength. The procedure appears promising and further numerical analysis on experimental data is necessary to validate the model.

6. Appendices

In a more general case when the NSIF is not known, the effective stress σ_{eff} can be calculated numerically by means of an FE code at any nodes of the mesh, by solving the Helmholz differential equation in volume V of the component by imposing Neumann boundary conditions [21]:

$$\sigma_{eff} - c^2 \nabla^2 \sigma_{eff} = \sigma_{eq} \qquad in \quad V \tag{A1}$$

In Eq. (A1) it is assumed that fatigue damage is due to the average, evaluated on the whole component, of a physical quantity called the equivalent stress σ_{eq} (for welded joints under proportional loading σ_{eq} agrees with the maximum principal stress σ_1) ∇^2 is the Laplace operator. Neuman boundary conditions are assumed: $\nabla\sigma_{eff} \cdot n = 0$ (where $\nabla\sigma_{eff}$ is the gradient of the effective stress). *c* is the characteristic length assumed as a material characteristic.

[1] *UNI EN 26520 (ISO 6520:1982)*, Classification of imperfections in metallic fusion welds
[2] *ISO 5817:2014 Welding* - Fusion-welded joints in steel, nickel, titanium and their alloys (beam welding excluded) - Quality levels for imperfections
[3] *ISO 10042:2018 Welding* -- Arc-welded joints in aluminium and its alloys -- Quality levels for imperfections
[4] Hobbacher A, 2007 Recommendations for fatigue design of welded joints and components. Paris, IIW: *International Institute of Welding, Document* XIII-1823e07/XV-1254-07
[5] BS 7608-2:1993. *Fatigue design and assessment of steel structures*
[6] Zerbs U T, Schödel M, Webster S, Ainsworth R, 2007 Fitness-for-Service Fracture Assessment of Structures Containing Cracks: *A Workbook based on the European SINTAP/FITNET procedure*, Elsevier, 1st ed. Oxford, Amsterdam, the Netherlands
[7] Miki C, Fahimuddin F, Faimuddin F, 2001 Fatigue performance of butt-welded joints containing various embedded defects *Struct. Mech. Earthquake Eng.*, JSCE, No. **668**/I-54
[8] *BS 7910:2005*. Guide to methods for assessing the acceptability of flaws in metallic structures
[9] Fomin F, Horstmann M, Huber N, Kashaev N, 2018 Probabilistic fatigue-life assessment model for laser-welded Ti-6Al-4V butt joints in the high-cycle fatigue regime. *International Journal of Fatigue* **116** pp 22-35
[10] Murakami Y, 2002 *Metal Fatigue: Effects of small defects and non-metallic inclusions*, Elsevier
[11] Schuscha M, Horvath M, Leitner M, Stoschka M, 2019 Notch Stress Intensity Factor (NSIF)-Based Fatigue Design to Assess Cast Steel Porosity and Related Artificially Generated Imperfections. *Metals* **9** pp 1097; doi:10.3390/met9101097
[12] Rigon D, Meneghetti G, 2020 An engineering estimation of fatigue thresholds from a microstructural size and Vickers hardness: application to wrought and additively manufactured metals. *International Journal of Fatigue* **139** https://doi.org/10.1016/j.ijfatigue.2020.105796
[13] Patriarca L, Beretta S, Foletti S, Riva A, Parodi S, 2020 A probabilistic framework to define the design stress and acceptable defects under combined-cycle fatigue conditions. *Engineering Fracture Mechanics* **224**, https://doi.org/10.1016/j.engfracmech.2019.106784
[14] Rizzoni R, Livieri P, Tovo R, Cova M, 2020 Development of a hierarchical model for voids clusters suitable for cast iron degenerated graphite. *Theoretical and Applied Fracture Mechanics*, **109**, 102731 https://doi.org/10.1016/j.tafmec.2020.102731
[15] Tovo R, Livieri P, 2007 An implicit gradient application to fatigue of sharp notches and weldments. *Engineering Fracture Mechanics* **74** pp 515–526
[16] Livieri P, Salvati E, Tovo R, 2016 A non-linear model for the fatigue assessment of notched components under fatigue loadings *International Journal of Fatigue*, **82**(3) pp 624–633
[17] Williams M L, 1952 Stress singularities resulting from various boundary conditions in angular corner of plates in extension. *ASME Journal of applied Mechanics* **19** pp 526–528
[18] Lazzarin P, Tovo R, 1998 A Notch Intensity Approach to the Stress Analysis of Welds. *Fatigue and Fracture of Engineering Materials and Structures* **21** pp 1089–1104
[19] Tovo R, Livieri P, 2008 An implicit gradient application to fatigue of complex structures, *Eng. Fract. Mech.*, **75** (7) pp 1804–1814
[20] Livieri P, Tovo R, 2020 Numerical predictions of the fatigue life of aluminium welded joints. *Procedia Structural Integrity* **26** pp 46–52 - https://doi.org/10.1016/j.prostr.2020.06.007
[21] Peerlings RHJ, de Borst R, Brekelmans WAM, de Vree JHP, 1996 Gradient enhanced damage for quasi-brittle material. *International Journal of Numerical Methods in Engineering* **39** pp 3391–3403
[22] Capetta S, Tovo R, Taylor D, Livieri P, 2011 Numerical Evaluation of Fatigue Strength on Mechanical Notched Components under Multiaxial Loadings. *International Journal of Fatigue*, **33** pp 661–671
[23] Livieri P, Meneghetti G, Tovo R, Volpone M, 2001 Defects influence on fatigue behaviour of laser welded joints, *8th INALCO 2001-International Conference on Joints in Aluminium*, Munich, Germany, 28-30 pp 4,3,1-4,3,10